In situ airborne measurements of aerosol optical properties during photochemical pollution events

M. Mallet, R. van Dingenen, Jean-Claude Roger, S. Despiau, H. Cachier

In situ airborne measurements of aerosol optical properties during photochemical pollution events

M. Mallet,[1] R. Van Dingenen,[2] J. C. Roger,[3] S. Despiau,[1] and H. Cachier[4]

Received 17 June 2004; revised 5 November 2004; accepted 22 November 2004; published 10 February 2005.

[1] Dry aerosol optical properties (scattering, absorbing coefficients, and single scattering albedo) were derived from in situ airborne measurements during two photochemical pollution events (25 and 26 June) observed during the Experience sur Site pour Contraindre les Modeles de Pollution atmospherique et de Transport d'Emissions (ESCOMPTE) experiment. Two flights were carried out during daytime (one during the morning and one at noon) over a domain, allowing the investigation of how an air pollution event affects the particle optical properties. Both horizontal distribution and vertical profiles are presented. Results from the horizontal mapping show that plumes of enhanced scattering and absorption are formed in the planetary boundary layer (PBL) during the day in the sea breeze–driven outflow of the coastal urban-industrial area of Marseille–Fos de Berre. The domain-averaged scattering coefficient (at 550 nm) over land σ_s changes from 35 (28) Mm^{-1} during land breeze to 63 (43) Mm^{-1} during sea breeze on 25 June (26 June), with local maxima reaching > 100 Mm^{-1}. The increase in the scattering coefficient is associated with new particle formation, indicative of secondary aerosol formation. Simultaneously, the domain-averaged absorption coefficient increases from 5.6 (3.4) Mm^{-1} to 9.3 (8.0) Mm^{-1}. The pollution plume leads to strong gradients in the single scattering albedo ω_o over the domain studied, with local values as low as 0.73 observed inside the pollution plume. The role of photochemistry and secondary aerosol formation during the 25 June case is shown to increase ω_o and to make the aerosol more 'reflecting' while the plume moves away from the sources. The lower photochemical activity, observed in the 26 June case, induces a relatively higher contribution of black carbon, making the aerosol more absorbing. Results from vertical profiles at a single near-urban location in the domain indicate that the changes in optical properties happen almost entirely within the PBL. No significant variation of σ_s, σ_a, and ω_o is observed in the upper layer (1–3 km), where the aerosol optical properties are considered to be well mixed.

Citation: Mallet, M., R. Van Dingenen, J. C. Roger, S. Despiau, and H. Cachier (2005), In situ airborne measurements of aerosol optical properties during photochemical pollution events, *J. Geophys. Res.*, *110*, D03205, doi:10.1029/2004JD005139.

1. Introduction

[2] Aerosol (or particulate matter) concentrations have increased significantly over the industrial period because of human activities. On the top of their health effect, aerosols are recognized to be a crucial agent of climate change [*Hansen et al.*, 2000]. However, in contrast with the radiative forcing due to greenhouse gases that may be determined to a reasonably high degree of accuracy, the uncertainties related to aerosol radiative forcings remain very large [*Intergovernmental Panel on Climate Change* (*IPCC*), 2001]. This is in the first place due to the complexity of aerosols: Atmospheric particles have different sizes, shapes, sources, chemical compositions and lifetimes, which makes it difficult to get an accurate global picture of the aerosol spatial and temporal distributions.

[3] At the present time, the major sources of data characterizing the aerosol properties are obtained from surface or remote sensing measurements. Owing to the complexity of the atmosphere vertical structure, ground-based measurements are not always representative of the whole atmospheric column [*Bergin et al.*, 2000]. On the other hand, the current remote sensing techniques from ground-based or satellite can only provide the properties of aerosol in entire atmospheric column [*Boucher and Tanré*, 2000; *Dubovik et al.*, 2000; *Kaufman et al.*, 2002]. Hence, in addition with such measurements, the necessity to perform systematic

[1]Laboratoire de Sondages Electromagnétiques de l'Environnement Terrestre–Laboratoire d'Etude des Echanges Particulaires aux Interfaces, UMR CNRS 6017, Université du Sud Toulon-Var, La Valette du Var, France.

[2]Climate Change Unit, Joint Research Center, Institute for Environment and Sustainability, European Commission, Ispra, Italy.

[3]Laboratoire en Océanographie Côtière et Littoral/Maison de la Recherche en Environnement Naturel, UMR CNRS ELICO 8013, Université du Littoral Côte d'Opale, Dunkerque, France.

[4]Laboratoire des Sciences du Climat et l'Environnement, Unité mixte CNRS-CEA, Gif sur Yvette, France.

0148-0227/05/2004JD005139

vertical (and horizontal) profile measurements from aircraft in selected regions is clearly needed [*Öström and Noone*, 2000; *IPCC*, 2001]. In addition, the aircraft observations provide unique information on vertical variability of aerosol properties as well as on aerosol properties in close vicinity of clouds. Such information is very hard to access from both ground-based and satellite observation while it is very important for analyzing radiative balance of the atmosphere and aerosol-cloud interaction.

[4] Aircraft observations were carried out during international experimental campaigns by *Collins et al.* [2000a] and *Öström and Noone* [2000] during ACE2 [*Raes et al.*, 2000], *de Reus et al.* [2002] during INDOEX [*Ramanathan et al.*, 2001] and *Hegg et al.* [1997] during TARFOX [*Hartley et al.*, 2000]. However, owing to the cost of airborne observations, in situ investigations of aerosol properties remain scarce. Furthermore, aircraft profiles are generally performed once during a given day in order to study a special aerosol event, such as dust particles transported into upper atmospheric layer, pollution particles over continental zone [*Collins et al.*, 2000b] or the mixing of the two [*Öström and Noone*, 2000]. These measurements provide crucial information on the distribution of aerosol properties but do not give access to their diurnal variation.

[5] The main objective of the present work is first to provide more knowledge about the vertical and horizontal distribution of particle optical properties in a continental polluted zone and, second, to investigate their diurnal evolution, in order to study how they could be affected by a photochemical pollution event. This work is based on vertical profiles and horizontal mapping of aerosol properties, performed during four flights (identified by flight numbers 41, 42, 43 and 44), on the 25 and 26 June of 2001, from nephelometer, Particle/Soot Absorption Photometer (PSAP), and number size distribution measurements, on board the Avion de Recherche et de Télédétection (ARAT) Fokker 27 aircraft during the ESCOMPTE field campaign [*Cros et al.*, 2004; *Cachier et al.*, 2005].

[6] The ESCOMPTE domain involves the urban area of Marseille and the industrial complex of Fos-Berre, located in the southeastern part of France, known as one of the most polluted sites in Europe. This region of France is subject to special meteorological conditions, leading to high and frequent pollution events, characterized by the development of an important anthropogenic aerosol plume. This high urban/industrial activity can also affect a large part of the region when pollutants are transported out of the source regions.

[7] We focused our studies on analysis on the total scattering (σ_s) and absorbing (σ_a) coefficients, but also on the aerosol single scattering albedo ω_o (ratio of total aerosol scattering to the sum of σ_s and σ_a), which is the key aerosol optical property dominating the aerosol radiative effect and which remains very difficult to estimate in all types of observation: from satellite [*Kaufman et al.*, 2002] and ground-based [*Dubovik et al.*, 2002] remote sensing as well as from in situ [*Russell et al.*, 2002] measurements.

2. Photochemical Event Studied: Intense Observation Period 2b (IOP2b)

[8] The IOP2b is presented in detail by *Cros et al.* [2004] and corresponds to the strongest photochemical pollution event observed during ESCOMPTE. During the 2 days used in this study (25 and 26 June), the wind was low, the temperature was above 34°C and the surface ozone concentration was about 100 ppbv or more over the whole domain (up to 150 ppbv in the Durance Valley on June 25; 115 ppbv in the Rhone valley on June 26). This photochemical event was extensively documented with six flights performed on 24, 25, and 26 June, respectively, and eight constant volume balloons launches (CVBs), four of them with an ozone probe.

3. Aircraft Flights

[9] Four ARAT (Fokker 27) flights, number 41 and 42 (25 June) and 43 and 44 (26 June) are investigated here, each including vertical ascents immediately after takeoff, between 0515–0537 UTC (41), 1032–1050 UTC (42), 0509–0529 UTC (43) and 1035–1055 UTC (44), respectively. The corresponding altitude ranges were 100–2586 m, 119–2846 m, 148–2872 m and 59–2843 m, for the four flights, respectively. After the vertical ascent, the aircraft performed also horizontal flights in the PBL for altitudes comprised between 400 and 1000 m, with typical flight patterns as illustrated in Figure 1. This allowed us to perform a domain mapping of the parameters measured on board the aircraft.

[10] The vertical sounding was located inland near the Avignon airport (43°90'N, 04°90'W), 50 km northwest of Berre industrial complex and 75 km away from Marseille (see *Cros et al.* [2004] and Figure 2). This continental site is often strongly affected by the pollution plume developed over the Marseille/Berre region. Indeed, the land breeze regime, characterizing each period of intensive observation during the day, is able to transport the pollution plume developed on the source in surrounding area.

4. Instrumentation

4.1. Aerosol Size Distribution Measurements

[11] Number size distributions in the diameter range 6–620 nm were measured with a Vienna-type medium size differential mobility analyzer (DMA), connected to a Condensation Particle Counter (TSI model 3010). The DMA drew, entering the common sample line via a semi-isokinetic inlet, its sample air out of a cylindrical buffer volume (18 L), which was continuously flushed using the aircraft's ram pressure. The DMA sheath air was circulated in a closed loop arrangement [*Jokinen and Mäkelä*, 1997] including a diffusion drier to keep humidity below 20%. The system was controlled in order to perform the distribution measurements in scanning mode (scan time: 50 s for a complete distribution measurement) [*Wang and Flagan*, 1990]. The accuracy of the DMA measurements is estimated to be within 15% for integrated number and 25% for integrated aerosol volume.

[12] The number concentration resulting from the DMA system agreed very well with the total number concentration measured with a parallel running TSI model 3022, even during vertical profiles with changing pressure (Figure 3). Hence distribution data obtained during the profiling

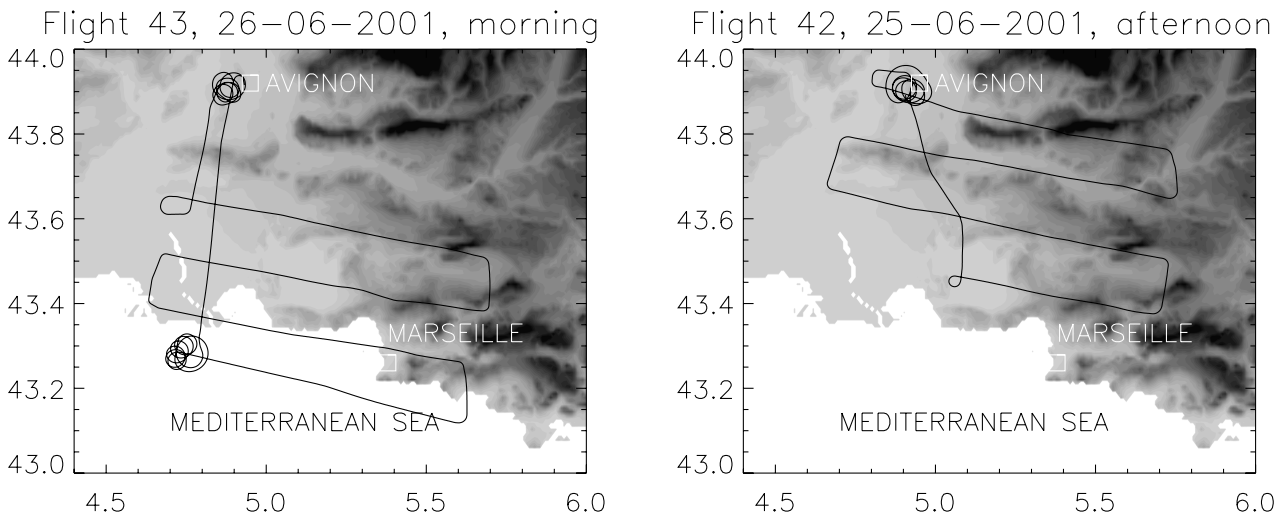

Figure 1. Typical flight patterns during 25 and 26 June.

ascents and descents were used to construct vertical profiles of the size distributions. Vertical profiles of number size distributions were retrieved on 25 and 26 June. On each of these days a morning and a noon flight was made, with typical flight patterns as shown in Figure 1. During the morning flight, vertical profiles were obtained over land (at the airport location) as well as off the coast. During the noon flight, only land was overflown. For 25 June, no size distribution data are available for the morning vertical profile over land.

4.2. Aerosol Optical Properties Measurements

4.2.1. Total Scattering Coefficient

[13] The total particle scattering coefficient σ_s in dry state, was measured at 450, 550 and 700 nm using a three-wavelength integrating nephelometer (TSI model 3563).

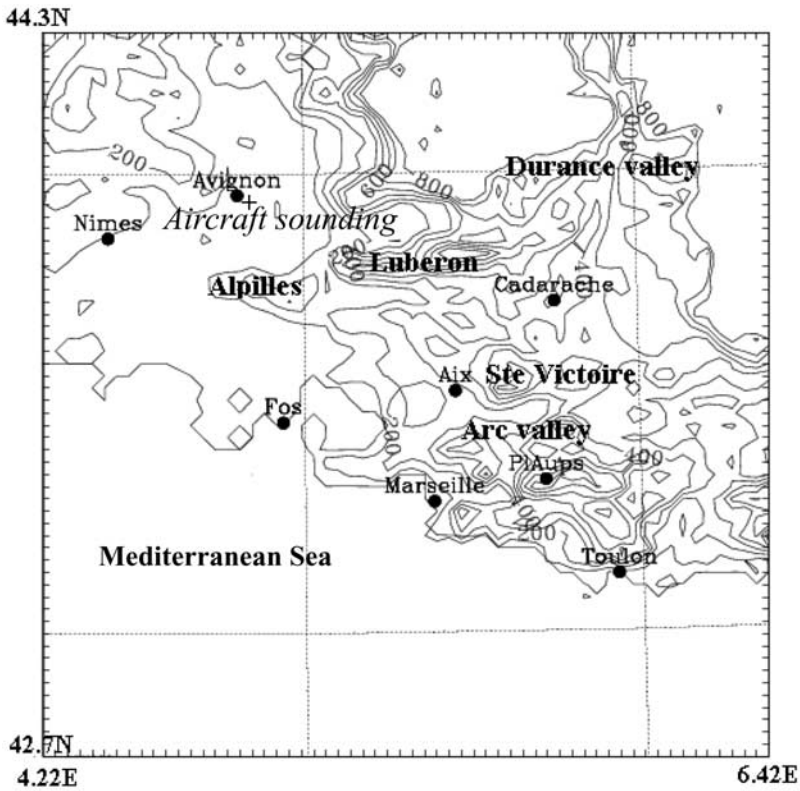

Figure 2. The aircraft sounding (near the city of Avignon) site indicated in the Experience sur Site pour Contraindre les Modeles de Pollution atmospherique et de Transport d'Emissions (ESCOMPTE) domain.

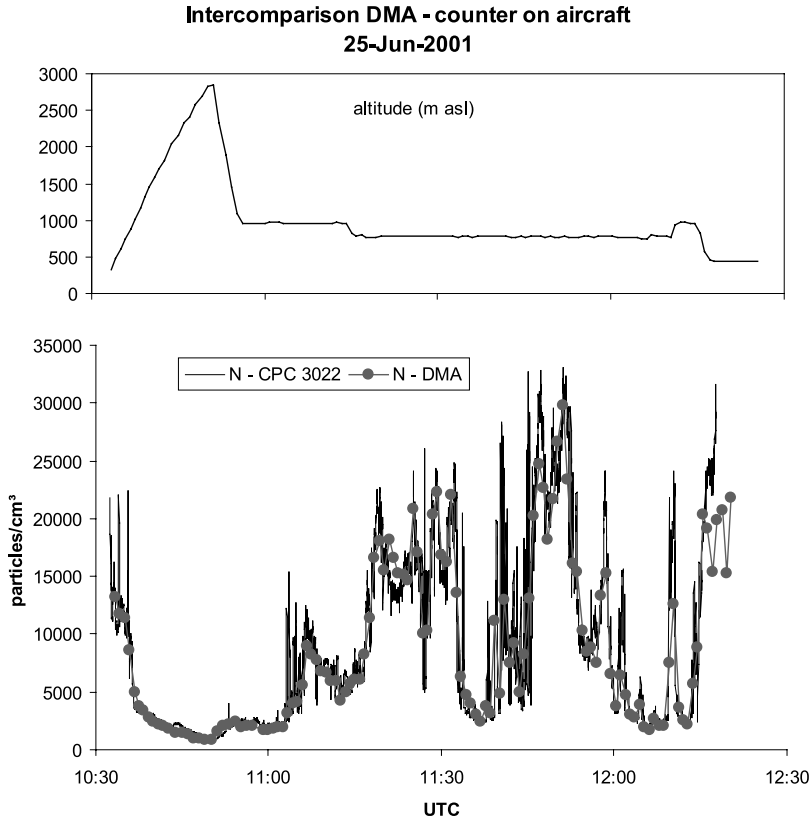

Figure 3. Number concentration resulting from the differential mobility analyzer (DMA) system compared to the total number concentration measured with a parallel-running TSI model 3022.

Air is sampled through the semi-isokinetic inlet and the sample relative humidity is maintained below 40%. The time resolution of the scattering coefficient measurement is about 1 s.

[14] One of the sources of errors from the nephelometer originates from the instrument geometrical limitations. Indeed, the integrating nephelometer cannot detect the entire phase function of the scattered light. It measures aerosol light scattering coefficient at two ranges of angular integration (7°–170°) and (90°–170°). Since the light scattered by the particles within the measurement chamber is only integrated between 7° and 170°, the results provided by the nephelometer measurements underestimate the actual total scattering coefficients. However, this effect has been shown to be low for anthropogenic submicronic aerosol. *Carrico et al.* [2000] reported an underestimation of the total scattering coefficient about $\sim$ 4% for anthropogenic aerosol, and *Formenti et al.* [2002] reported a total correction factor ranging between 1.08 and 1.05 (from 450 to 700 nm) for an aerosol characterized by a modal diameter around 0.15 μm. In this study, we applied the correction factor given by *Anderson et al.* [1999] for the data presented here.

[15] The total scattering coefficient, σ_s has been estimated as

$$\sigma_s = \sigma_{ns} C_{s,\mathrm{ang}} \quad (1)$$

where σ_{ns} is the nephelometer measurement and $C_{s,\mathrm{ang}}$ is the correction factor for nephelometer angular nonidealities. *Anderson et al.* [1999] showed that $C_{s,\mathrm{ang}}$ can be estimated from the wavelength dependence of light scattering, as measured by the nephelometer, and they proposed the following relation:

$$C_{s,\mathrm{ang}} = A_1 + A_2 \alpha \quad (2)$$

where α is the measured Angstrom exponent. The values of the A_1 and A_2 coefficients are reported by *Anderson et al.* [1999]. Our computations showed that $C_{s,\mathrm{ang}}$ ranged between 1.13 and 1.14 for each day investigated in the present study.

4.2.2. Total Absorption Coefficient and Single Scattering Albedo

[16] The Particle Soot Absorption Photometer (PSAP, Radiance Research) was used to measure in quasi-real time the light absorption coefficient, σ_a, at 567 nm. As the PSAP time resolution is 5 s, nephelometer measurements were averaged on 5 s in order to combine the two optical measurements.

[17] The PSAP absorption method is based on the integrating plate technique by which the change in optical transmission of a filter caused by particle deposition is related to the light absorption coefficient, of the deposited particles, using Beer's law. Errors on the PSAP measurements can arise from the unit to unit variability, instrumental noise, inaccurate knowledge of operational parameters (filter spot size and airflow rate), scattering particles being misinterpreted as absorption and overestimate of absorption from multiple scattering. The largest error (around 22%) is

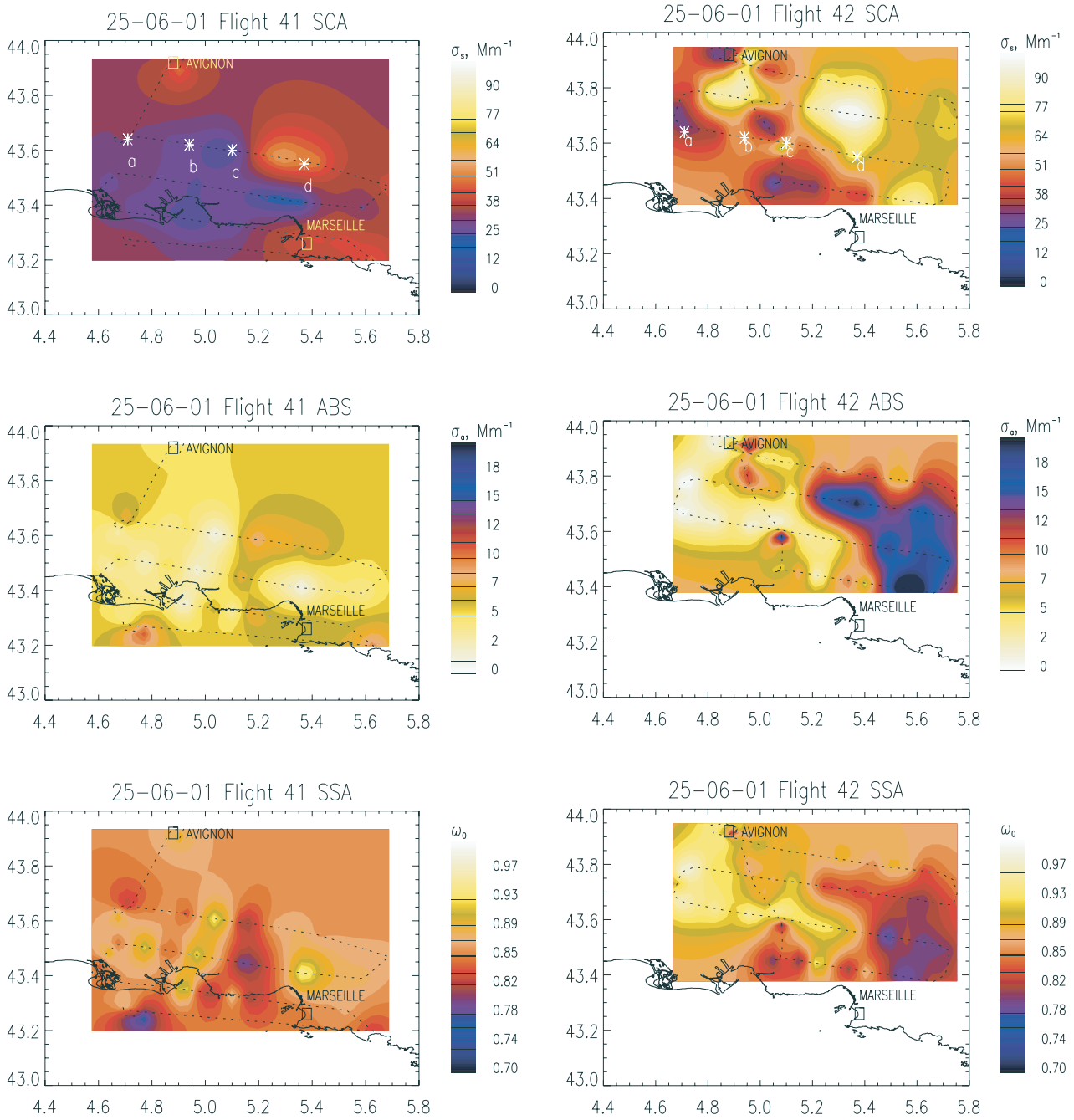

Figure 4. Horizontal distribution of the scattering (SCA), absorption (ABS), and single scattering albedo (SSA) on the whole ESCOMPTE domain for the 25 June case.

due to misinterpretation of multiple scattering as absorption. Source for errors are detailed by *Bond et al.* [1999] and may be quantified in the following equation:

$$\sigma_{a\_\text{corrected}} = \left(\sigma_{\text{adj}} - K_1\sigma_s\right)/K_2 \tag{3}$$

where $\sigma_{a\_\text{corrected}}$ is the absorption coefficient corrected from all the sources of errors. σ_{adj} is the coefficient corrected from the flow rate and area. K_1 is equal to 0.02, σ_s is the total scattering coefficient (corrected from angular nonidealities) measured from nephelometer and K_2 is equal to 1.22.

[18] The combination of the aerosol total scattering coefficient, σ_s, and the absorption coefficient, σ_a, allows the estimation of the dry aerosol single scattering albedo, using the following relation:

$$\omega_o = \sigma_s/(\sigma_s + \sigma_a) \tag{4}$$

5. Results and Discussion

5.1. Distribution and Evolution of Aerosol Parameters in the PBL

[19] By applying kriging interpolation, the parameters measured during the legs flown as shown in Figure 1, can be plotted for the whole domain. Figures 4 and 5 show the

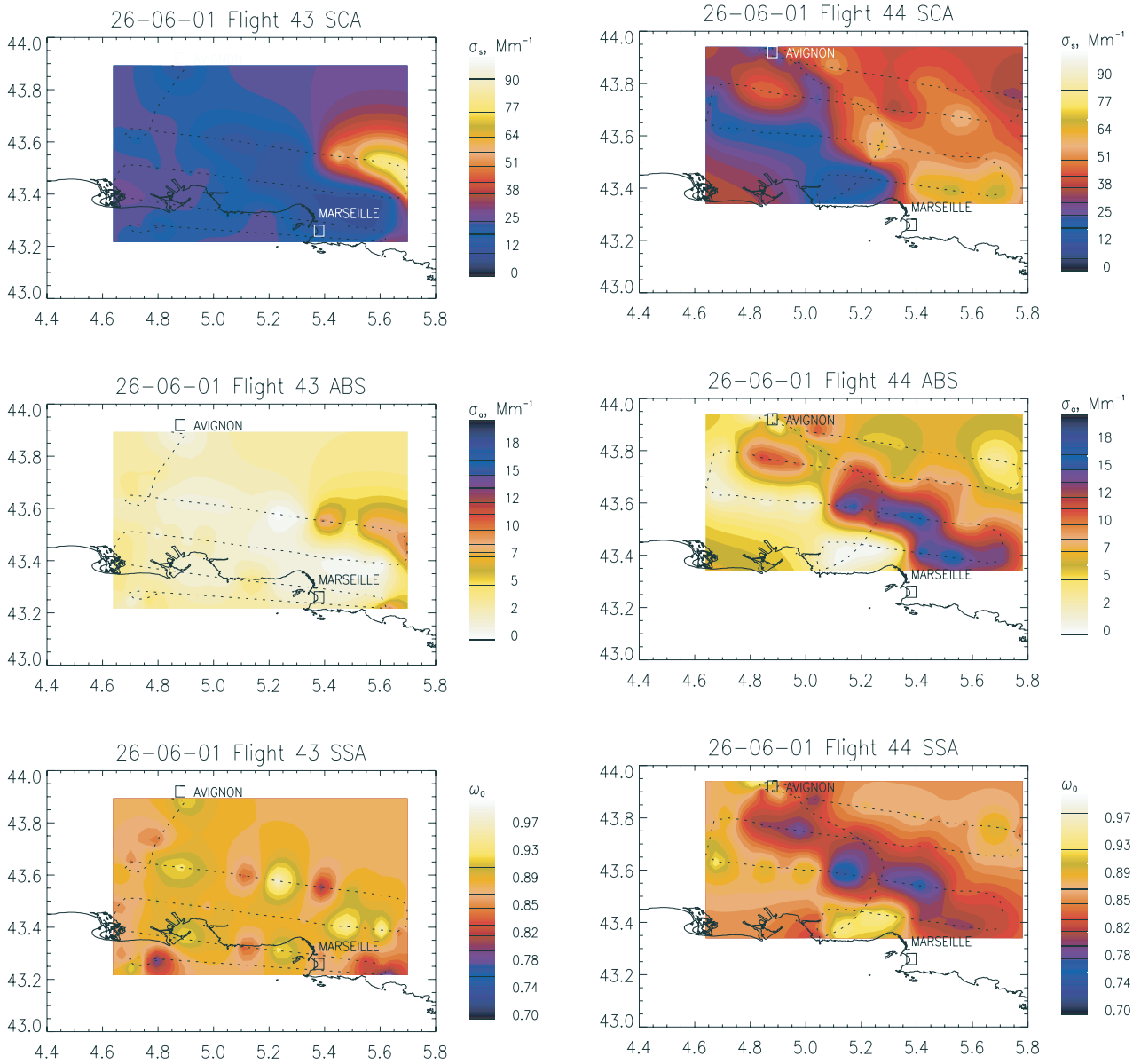

Figure 5. Horizontal distribution of the SCA (scattering), ABS (absorption), and SSA (single scattering albedo) on the whole ESCOMPTE domain for the 26 June case.

results for the aerosol optical properties (scattering (SCA), absorption (ABS) and single scattering albedo (SSA) at 550 nm) for the 2 days studied here. Despite the uncertainties associated with such interpolation, some interesting observations can be made.

[20] For 25 June (Figure 4), comparisons between morning and noon indicate clearly the appearance of a very strong scattering ($\sigma_s > 100$ Mm^{-1}) and absorbing ($\sigma_a \sim 20$ Mm^{-1}) plumes at noon. This coincides with the observation of high O_3 levels for this day (100 ppbv over the whole domain and up to 150 ppbv in the Durance Valley [see *Cros et al.*, 2004]). We also note a strong similarity in the geographical patterns of the plumes, both for absorption and scattering, indicating that they are originating in the urban-industrial area around Marseille, and transported land inward with the sea breeze that has developed by noon. This photochemical event, observed during 25 June, creates very high value of the scattering coefficient, with $\sigma_s > 100$ Mm^{-1} in the plume maximum. Although the absorption was also quite high ($\sigma_a \sim 20$ Mm^{-1} in the urban plume of Marseille, presumably because of black carbon production from traffic), the single scattering albedo remains relatively high on the whole ESCOMPTE domain ($\omega_o > 0.90$), because of the high scattering, except inside the urban plume ($\omega_o \sim 0.85$).

[21] The trend in scattering coefficient can be related to changes in the number size distribution. Figure 6 shows the distributions on the four locations indicated on Figure 4 during morning and noon flight of 25 June, respectively. It can be seen that the increase in scattering coefficient is associated with both an increase in the accumulation mode as well as in the nucleation mode, in particular at the edge of the high scattering plume (Figure 6d). The presence of a fresh nucleation mode, together with the occurrence of the maximum scattering downwind of the source area suggests

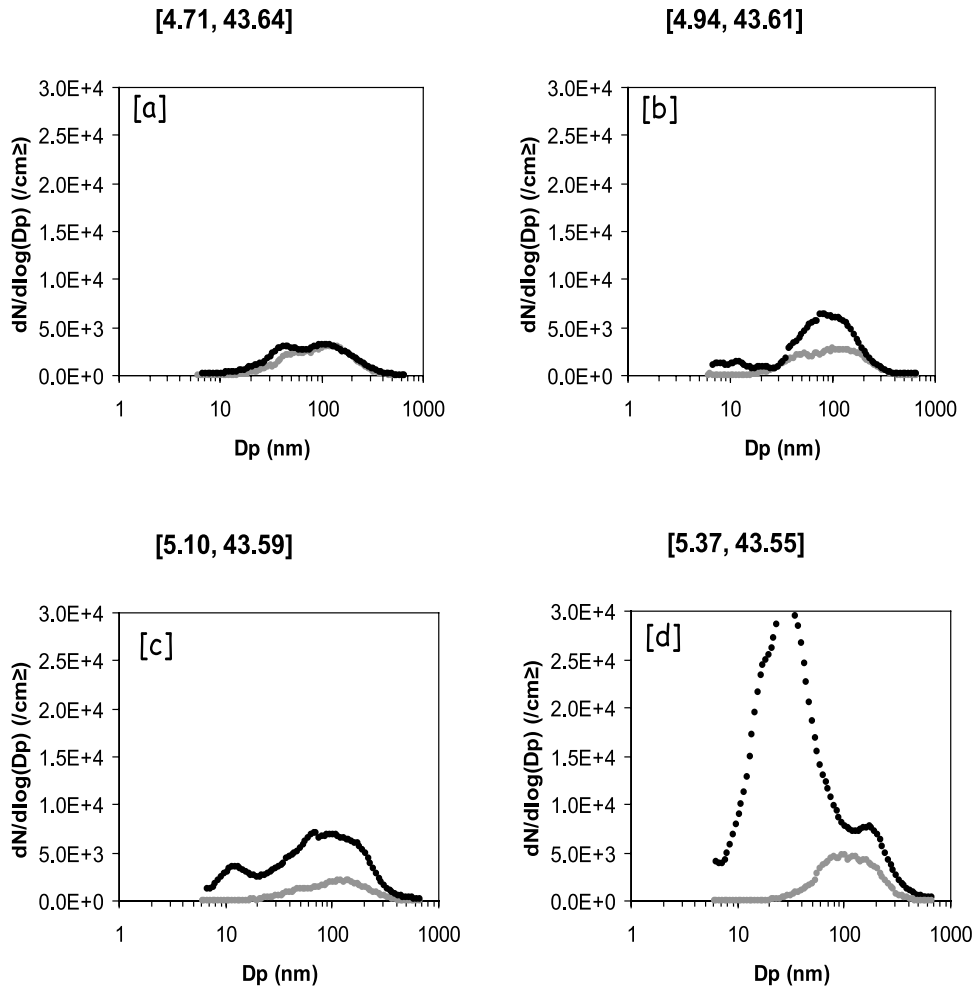

Figure 6. Number size distributions (a, b, c, and d) on four locations indicated on Figure 4 during morning (grey dots) and noon (solid dots) 25 June flights.

that much of the increased scattering is due to the production of secondary aerosol.

[22] Concerning 26 June, the situation is quite different; photochemistry is not so prominent and we note a much lower scattering compared to the day before (with $\sigma_s \sim 20\ \mathrm{Mm}^{-1}$ and $60\ \mathrm{Mm}^{-1}$, outside and inside the urban plume, respectively). Although less pronounced than for 25 June noon, we note a relatively high absorption coefficient in the urban plume leading to quite some gradients in the single scattering albedo at noon, with lower values ($\omega_o \sim 0.75$) than for 25 June in the plume (Figure 5).

[23] We computed the averaged value of optical parameters, aerosol number and volume (Table 1) in the PBL for the whole ESCOMPTE domain from horizontal measurements, between 500 and 1000 m altitude. The averaged data confirm the strong increase in scattering and absorption at noon of the 2 days studied. During the night, the land breeze system cleans the area and brings levels of all "extensive" aerosol parameters down. One of the interests here concerns the evolution of the single scattering albedo ω_o between morning and noon. The 25 June case shows that the pollution plume does not strongly modify ω_o from morning to noon, hence keeping the aerosol reflecting and thus more "cooling" for the Earth-atmosphere system. In fact, despite the outflow of an absorbing plume from the urban area (Figure 4, flight 42 ABS), the production of scattering material from secondary aerosol formation compensates the absorbing BC aerosol production from traffic. It is indeed interesting to note that the "central blob" around coordinates (43.7, 5.35) of the absorption plume turns out to have a higher single scattering albedo (SSA plot, Figure 4) than the part of the plume near Marseille. The former seems to be developed some distance away from the source as aerosols need time to grow in order to become effectively scattering. This indicates also the role of the secondary aerosol formation to make an absorbing plume "more scattering."

[24] During 26 June, because of the lower photochemistry, the contribution of BC is relatively higher, and hence the aerosol becomes more absorbing ($\omega_o \sim 0.89$ in the morning, $\omega_o \sim 0.86$ at noon), which could lead to a "semidirect" effect at the regional scale. This effect can induce a nonnegligible heating rate of the PBL, as shown by *Roger et al.* [2002] at the Vallon Dol site, changing the atmospheric stability. We can also observe strong horizontal heterogeneity in ω_o (Figure 5), with remarkable different "hot" spots, where ω_o reaches the value of 0.74, in particular at noon on 26 June.

Table 1. Overview of Domain-Averaged Aerosol Parameters in the PBL Over Land During IOP2b Measured From the ARAT Research Aircraft, Based on 1 min Averaged Values[a]

	25 June Morning Flight 41	25 June Noon Flight 42	26 June Morning Flight 43	26 June Noon Flight 44
		Green Scattering Coefficient σ_s, Mm^{-1}		
Average	35.6	63.0	28.0	42.9
Standard deviation	8.9	22.3	19.9	17.5
Minimum	23.4	23.9	12.2	13.5
Maximum	59.9	116.4	91.8	77.3
		Absorption Coefficient σ_a, Mm^{-1}		
Average	5.6	9.3	3.4	8.0
Standard deviation	2.3	6.4	2.9	5.1
Minimum	0.8	0.2	0.1	0.2
Maximum	12.6	24.2	12.1	18.4
		Single Scattering Albedo ω_0		
Average	0.87	0.88	0.89	0.86
Standard deviation	0.04	0.06	0.04	0.05
Minimum	0.75	0.76	0.77	0.73
Maximum	0.97	1.00	1.00	0.99
		Aerosol Number Concentration N, cm^{-3}		
Average	2625	9630	1801	10175
Standard deviation	1060	6759	947	7604
Minimum	1405	1740	1037	1414
Maximum	6666	26667	6109	31370
		Aerosol Volume Concentration ($D < 1$ μm) V, $\mu m^3\ cm^{-3}$		
Average	6.3	16.9	6.4	10.1
Standard deviation	2.7	7.7	3.7	4.1
Minimum	3.5	4.4	2.4	3.2
Maximum	14.2	33.9	22.5	20.8

[a]PBL is planetary boundary layer (700 m < altitude < 1000 m). IOP2b is intense observation period 2b. ARAT is Avion de Recherche et de Télédétection.

[25] The highest level of pollution is reached at noon on 25 June, where σ_s reaches the average value of 63 Mm^{-1} (Table 1) and locally even 100 Mm^{-1} (Figure 4). This value is found to exceed values observed in different strongly polluted zones. For example, during ACE-Asia, *Anderson et al.* [2003] performed measurements of aerosol optical properties over the Pacific on board of the C-130 aircraft and reported a mean value of dry σ_s equal to 55 Mm^{-1} for the fine-mode anthropogenic aerosol, majority located in the boundary layer. Similar observations have been made concerning the INDOEX experiment, where *de Reus et al.* [2002] indicated a dry scattering coefficient about 70 Mm^{-1} close to pollution source of the Indian subcontinent. Although depending on the site of measurements, the σ_s values reported above have been observed in the plume of important sources of anthropogenic aerosol (Asia continent, Indian continent), and this intercomparison shows clearly the high level of pollution observed on the region of Marseille and Etang de Berre.

[26] Assuming a density of 1.5 g cm^{-3} for the submicron aerosol (as derived from ground-based gravimetric impactor and DMA data during the same campaign (Figure 7) [*Van Dingenen et al.*, 2002]), we derive from the domain-averaged scattering coefficient and aerosol volume, a dry mass scattering efficiency for the PBL between 2.5 and 3.8 $m^2\ g^{-1}$, which is in the range of values observed for continental aerosol (3.5 $m^2\ g^{-1}$ for "continental polluted aerosol" [*IPCC*, 2001]), providing an additional quality check on the data.

[27] The lowest value for the single scattering albedo is observed at noon on 26 June (ω_o = 0.73). This value is rather low, but again coherent with the one reported by *Formenti et al.* [2002] during STAAARTE-MED (0.75 ~ 0.80 at 550 nm), which took place over Greece and parts of the Mediterranean Sea during August 1998 during a profile descent in northeastern Greece. We report from the latter study the value of ω_o measured in the boundary layer (0–1000 m) and not the one measured for the layer above, located between 1.5 and 3 km and demonstrated by *Formenti et al.* [2002] to be composed by an aged biomass burning plume. Our value of ω_o is, however, still larger than the one measured during INDOEX (~0.6 at 550 nm) by *de Reus et al.* [2002], because of the higher black carbon mass percentage (~ 14%) on the submicron aerosol [*Ramanathan et al.*, 2001].

5.2. Vertical Profiles of Aerosol Parameters

[28] In this section we explore the vertical distribution of aerosol parameters measured during the spiraling vertical ascent flight patterns (see Figure 1). The profiling over land took place near the airport of Avignon; hence PBL data may be influenced by local urban emissions, in particular for the noon flight. The upper layer data, however, can be assumed to be more representative for the area. Vertical profiles of aerosol number concentration, scattering coefficient and single scattering albedo for the four flights are shown in Figure 8. Table 2 summarizes averaged aerosol data for the upper layer, i.e., the part of the vertical profile higher than 1000 m. Table 2 shows that in the upper layer (UL), contrary to the PBL, little difference is observed between morning and noon flights, with morning values for all parameters corresponding well to those in the PBL. We

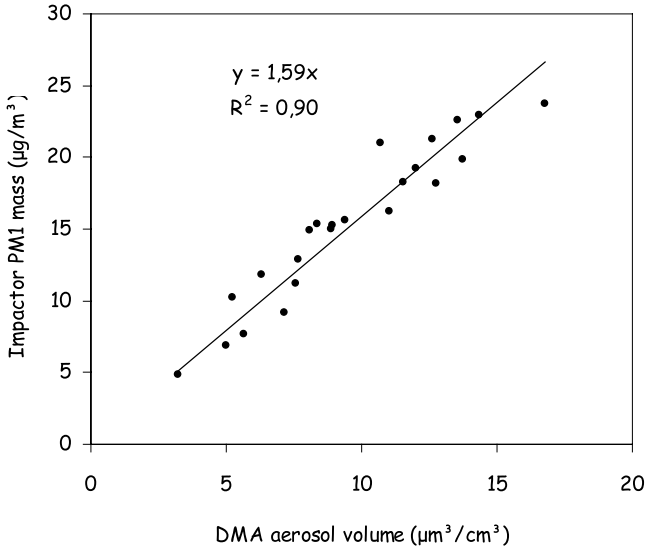

Figure 7. Correlation between aerosol volume (from DMA size distributions) and gravimetric mass on the impactor stages corresponding to the DMA size range.

will discuss now in more detail the vertical profiles for the various aerosol parameters.

5.2.1. Vertical Profile of Total Scattering Coefficient, σ_s

5.2.1.1. Research Flights 41 and 42, 25 June 2001

[29] During the vertical ascent of the flight 41, carried out during the morning of 25 June, the averaged σ_s is equal to 63 Mm^{-1} in the PBL at the location of the profile, and 48 Mm^{-1} in the upper layer (800–3000 m) at 550 nm. This σ_s vertical gradient is consistent with the higher aerosol volume observed in the PBL ($V \sim 15$ μm^3 cm^{-3}) compared to UL ($V \sim 7$ μm^3 cm^{-3}).

[30] During the vertical ascent of flight 42, performed at noon, the mean total scattering coefficient was about 90 Mm^{-1} in the PBL, with high variability and higher values around 500 m, indicating an important increase of σ_s (Figure 8) compared to the value obtained during the morning. As discussed in the previous section, the increase of σ_s in the PBL is due to the development of a photochemical event during 25 June, clearly indicated in Figure 8, leading to an increase of the aerosol concentration in PBL.

[31] Although no size distribution data are available in the morning from the vertical profile over land, DMA measurements from the horizontal leg near Avignon show a rather uniform unimodal size distribution (Figure 9), with one (accumulation) mode centered around 100 nm, similar to the morning distributions (grey dots) shown in Figure 6. At noon (see Figure 10), the number size distributions indicate an increase of the accumulation mode but also of the nucleation mode (centered around 10–20 nm), indicating clearly the effect of photochemical activity on the (secondary) aerosol production. This spectacular increase of the submicron aerosol concentration in the PBL at noon changes the scattering efficiency of the PBL (see Figure 8), leading to higher σ_s ($\sim$90 Mm^{-1}) compared to the morning ($\sim$60 Mm^{-1}). In the UL, however, no significant difference in σ_s is found between morning and noon ($\sim$45 Mm^{-1}). Indeed, the main modifications on the aerosol size distribution and concentration are observed in the PBL and not in the UL, where a unimodal (accumulation mode) number size distribution still prevails, with no important change in aerosol concentration between morning and noon (Figure 10).

5.2.1.2. Research Flights 43 and 44, 26 June 2001

[32] As observed for 25 June, the σ_s vertical profile obtained for flight 43 (morning) indicates a vertical gradient between PBL and UL, with higher scattering in the PBL, especially in the low atmosphere (0–500 m), where σ_s reaches the value of 77 Mm^{-1}. The averaged σ_s is about 30 Mm^{-1} in the UL, with higher values in the layer between 1500 and 1650 m.

[33] For the vertical ascent of flight 44 (noon), we observe an important increase of σ_s in the PBL with a mean value around 50 Mm^{-1}. The σ_s augmentation is mainly observed in the atmospheric layer between 400 and 1000 m, as shown in Figure 8. As it was the case for 25 June, the augmentation of scattering is due to the development of a photochemical episode, leading to an increase of anthropogenic particles concentration in PBL. Indeed, on 26 June the noon number size distribution shows a spectacular increase in the nucleation and Aitken mode (Figure 10), indicating secondary aerosol formation associated with high photochemical activity.

[34] Concerning the UL, σ_s remains still constant ($\sim$ 30 Mm^{-1}) along 26 June. This is well coherent with the DMA measurements, indicating that particle formation is clearly confined to the boundary layer and drops sharply to background levels above 1300 m (Figure 10), where a unimodal size distribution is observed both in the morning and noon.

5.2.2. Vertical Profile of Single Scattering Albedo, ω_o

5.2.2.1. Research Flights 41 and 42, 25 June 2001

[35] The dry ω_o vertical profiles during the flights 41 and 42 are reported in Figure 8. Compared to the nephelometer which was measuring between 100 and 3000 m, the PSAP (Particle Soot Absorption Photometer) measurements were performed for these altitudes between 500 and 3000 m. Hence the dry single scattering albedo was calculated for these altitudes, averaging the nephelometer data over the time needed for each PSAP measurement (5 s). As mentioned in section 1, one of the interests here is to study how the air pollution event affects the aerosol single scattering albedo, which represents one of the key optical properties with respect to the direct radiative effect of aerosol [*Russell et al.*, 2002].

[36] Concerning flight 41, we observe that the mean ω_o is higher in the PBL ($\omega_o \sim 0.94$) than the one measured in the UL ($\omega_o \sim 0.87$). As the absorbing coefficient σ_a is quite similar for both atmospheric layers ($\sigma_a \sim 8$ Mm^{-1}), the difference observed is due to higher σ_s measured in the PBL (63 Mm^{-1}) compared to the UL (49 Mm^{-1}).

[37] As we can see on Figure 8, a well-defined layer, responsible for the lower ω_o value in the PBL, clearly appears between 750 and 850 m. At these altitudes, ω_o is between 0.55 and 0.69 with a mean ω_o of 0.60. Into this layer, an important aerosol atmospheric direct effect could appear, leading to an increase of the local temperature, what can also change the convective circulation, evaporation processes or cloud formation.

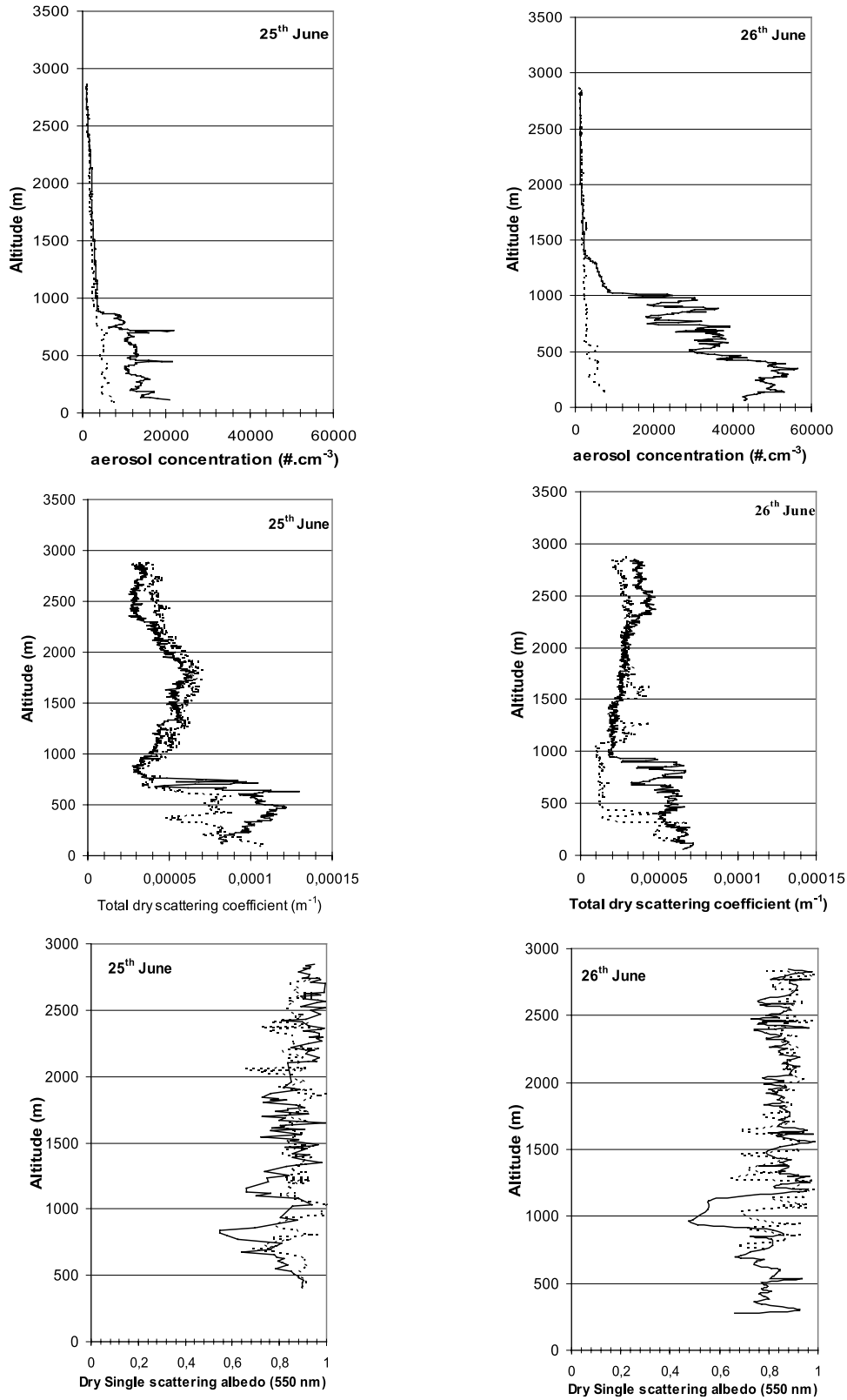

Figure 8. Vertical profiles of aerosol number concentration, dry total scattering coefficient σ_s, and dry aerosol single scattering albedo ω_o at 550 nm for the four flights. Dashed lines correspond to the morning flight; solid lines correspond to the noon flights.

Table 2. Overview of Profile-Averaged Aerosol Parameters in the UL During IOP2b Measured From the ARAT Research Aircraft, Based on 1 min Averaged Values[a]

	25 June Morning Flight 41	25 June Noon Flight 42	26 June Morning Flight 43	26 June Noon Flight 44
		Green Scattering Coefficient σ_s, Mm^{-1}		
Average	43.3	46.6	28.6	28.3
Standard deviation	9.7	11.4	5.6	7.2
Minimum	30.3	29.8	14.8	20.1
Maximum	64.2	65.3	40.8	42.2
		Absorption Coefficient σ_a, Mm^{-1}		
Average	5.7	4.0	3.3	3.6
Standard deviation	2.2	2.9	1.4	1.7
Minimum	1.7	0.9	0.1	1.2
Maximum	11.6	9.7	6.7	7.6
		Single Scattering Albedo ω_0		
Average	0.88	0.93	0.90	0.89
Standard deviation	0.04	0.04	0.04	0.04
Minimum	0.76	0.86	0.82	0.78
Maximum	0.95	0.97	1.00	0.95
		Aerosol Number Concentration N, cm^{-3}		
Average	1751	1846	1721	2336
Standard deviation	776	819	513	1978
Minimum	843	812	1001	845
Maximum	4225	3727	2781	9149
		Aerosol Volume Concentration ($D < 1$ μm) V, $\mu m^3\ cm^{-3}$		
Average	6.7	6.4	3.4	3.6
Standard deviation	4.1	3.8	1.3	1.6
Minimum	1.8	2.1	1.4	1.4
Maximum	16.9	14.2	7.3	6.8

[a]UL is upper layer (altitude > 1000 m).

[38] We observed a difference in ω_o in the PBL between morning ($\omega_o \sim 0.94$) and noon ($\omega_o \sim 0.78$) due to the stronger increase of the absorption coefficient σ_a (for the profile near Avignon by as much as a factor of 2.6), compared to the scattering coefficient σ_s (by a factor of 1.4), leading to a decrease of ω_o. Contrary to the variation observed in the PBL, ω_o does not vary in the UL between the morning and noon, as no change is observed on the scattering and absorbing coefficient values, which remain still constant ($\sigma_s \sim 45$ Mm^{-1}, $\sigma_a \sim 7$ Mm^{-1}). This leads to an important ω_o vertical gradient at noon, at the location of the vertical ascent, where ω_o appears higher in the elevated layer ($\omega_o \sim 0.88$), compared to the boundary layer ($\omega_o \sim 0.78$). AERONET retrieval (at 0600 UTC) of the single scattering albedo at Avignon indicated a coherent value ($\omega_o \sim 0.93$ at 550 nm) compared to the one obtained from optical measurements for flight 41 (0515–0537 UTC, $\omega_o \sim 0.94$ in the PBL).

5.2.2.2. Research Flights 43 and 44, 26 June 2001

[39] The ω_o vertical profile analysis for flights 43 and 44 indicates the same behavior as the one observed for 25 June. Indeed, while no variation clearly appears for the single scattering albedo in the UL (~0.87), the measurements performed in the PBL indicate a change in ω_o between morning (~0.82) and noon (~0.76). As observed for flight 42, a well-defined layer, with low ω_o values, clearly appears in the PBL, between 900 and 1100 m, close to the one observed for flight 42. At this altitude, ω_o is between 0.49 and 0.56 with a mean value of 0.53. As was the case for 25 June, this diminution of ω_o observed at noon is due to an increase of σ_a by as much as a factor of 5, between morning (~3 Mm^{-1}) and noon (~15 Mm^{-1}), while σ_s increases only by as much as a factor of 2 (26 Mm^{-1} in the morning and 54 Mm^{-1} at noon).

6. Conclusion

[40] The main objective of the present work was to investigate how the optical properties of particles are affected during an important photochemical event. Our work is based on data collected during four successful flights, numbers 41 and 42 (25 June) and 43 and 44 (26 June), performed during a strong pollution event (IOP2b) during the ESCOMPTE experiment [*Cros et al.*, 2004; *Cachier et al.*, 2005]. Results presented here are focused on the aerosol scattering, absorption coefficient, and the associated single scattering albedo. Both horizontal distribution and vertical profiles are presented.

[41] Horizontal maps of the optical properties in PBL indicate clearly the appearance of a very strong scattering and absorbing plumes at noon, produced from the urban-industrial area around Marseille, and transported land inward with the sea breeze that has developed by noon. The domain-averaged scattering coefficient (at 550 nm) over land σ_s changes from 35 (28) Mm^{-1} during land breeze to 63 (43) Mm^{-1} during sea breeze on 25 June (26 June). The 25 June photochemical event creates very high value of the scattering coefficient, with $\sigma_s > 100$ Mm^{-1} in the plume, superior in magnitude to the one observed in different strongly polluted zones (ACE-Asia, INDOEX), indicating the high level of pollution. The augmentation of

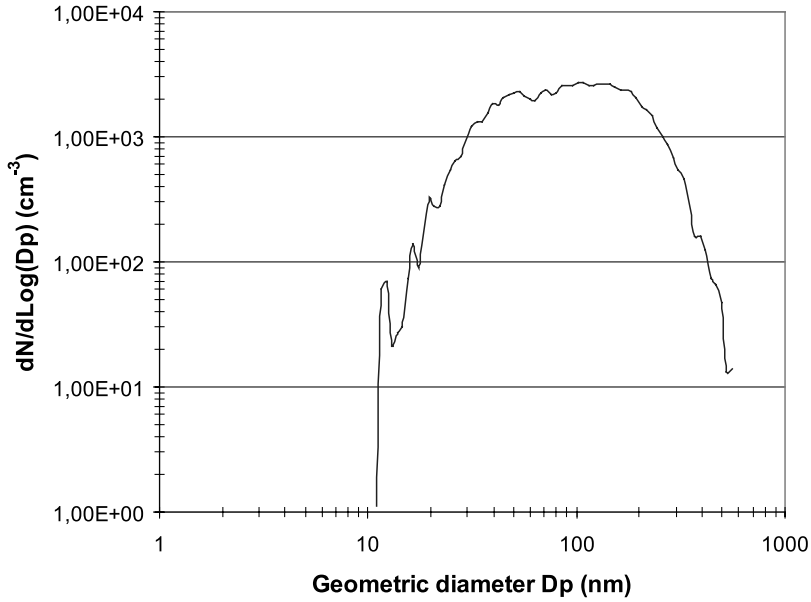

Figure 9. Aerosol number size distribution measured from DMA for flight 41 at 43°62′N, 04°94′W (0548 UTC, altitude of 764 m).

scattering is due to the development of a photochemical episode, leading to an increase of secondary anthropogenic particle concentration in the PBL. Simultaneously, the domain-averaged absorption coefficient increases from 5.6 (3.4) Mm^{-1} to 9.3 (8.0) Mm^{-1}. We observed strong horizontal heterogeneity in ω_o, with local values as low as 0.73 inside the pollution plume.

[42] The role of photochemistry and secondary aerosol formation during the 25 June case is clearly shown to increase ω_o and to make the aerosol more 'reflected.' On

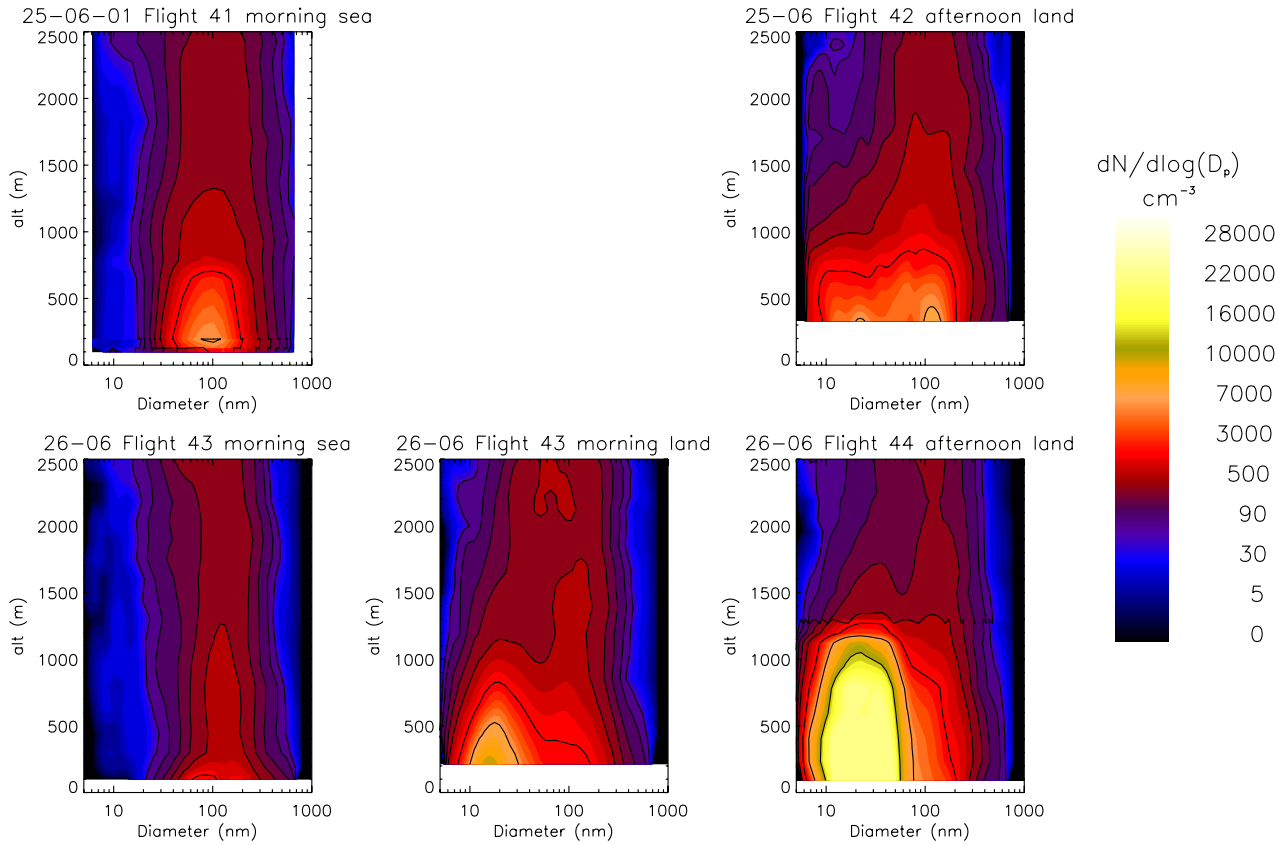

Figure 10. Vertical profile of the aerosol number size distribution measured from differential mobility analyzer.

the contrary, the lower photochemistry activity observed in the 26 June case induces a relatively higher contribution of black carbon aerosols, making the aerosol more absorbing, which can also lead to a nonnegligible "semidirect" effect at the regional scale.

[43] Results from vertical profiles at a single near-urban location (43°90′N, 04°90′W) indicated that the changes in optical properties happen almost entirely within the PBL. For example, the scattering coefficient σ_s strongly increased between morning and noon for the two cases investigated, leading to an important σ_s vertical gradient at noon, where the PBL appeared more efficient at scattering light than the elevated layer.

[44] **Acknowledgments.** The authors are indebted to Bernard Cros and Pierre Durand for the organization of the ESCOMPTE experiment. They gratefully thank the different Institutes in France (CNRS, INSU, ADEME, Ministry of Environment) for their support. Logistic help from local agencies (AIRMAREX and AIRFOBEP) is gratefully acknowledged. We would also like to thank P. Perros and S. Alfaro for their help concerning the TSI nephelometer and we also thank the ARAT F27 staff (PI: A. Gribkoff and C. P. Allet) for the data collection. Part of the ARAT flight hours have been funded through the EU programme for 'Coordinated Access to Aircraft for Transnational Environmental Research' (CAATER), subproject 'AEROPLUM.' We gratefully acknowledge the contribution of G. Penazzi as INSU/ARAT Fokker 27 Facilitator.

References

Anderson, T. L., D. S. Covert, J. D. Wheeler, J. M. Harris, K. D. Perry, B. E. Trost, D. J. Jaffe, and J. A. Ogren (1999), Aerosol backscatter fraction and single scattering albedo: Measured values and uncertainties at a coastal station in the Pacific Northwest, *J. Geophys. Res.*, *104*, 26,793–26,807.

Anderson, T. L., et al. (2003), Variability of aerosol optical properties derived from in situ aircraft measurements during ACE-Asia, *J. Geophys. Res.*, *108*(D23), 8647, doi:10.1029/2002JD003247.

Bergin, M. H., S. E. Schwartz, R. N. Haltore, J. A. Ogren, and D. L. Hlavka (2000), Comparison of aerosol optical depth inferred from surface measurements with that determined by Sun photometer for cloud-free conditions at a continental U.S. site, *J. Geophys. Res.*, *105*, 6807–6816.

Bond, T. C., T. L. Anderson, and R. J. Charlson (1999), Calibration and intercomparison of filter-based measurements of visible light absorption by aerosols, *Aerosol Sci. Technol.*, *30*, 582–600.

Boucher, O., and D. Tanré (2000), Estimation of the aerosol perturbation to the Earth's radiative budget over oceans using POLDER satellite aerosol retrievals, *Geophys. Res. Lett.*, *27*, 1103–1105.

Cachier, H., et al. (2005), Aerosol studies during the ESCOMPTE Experiment: An overview, *Atmos. Res.*, in press.

Carrico, C. M., M. J. Rood, J. A. Ogren, C. Neusüß, A. Wiedensohler, and J. Heintzenberg (2000), Aerosol optical properties at Sagres, Portugal, during ACE 2, *Tellus, Ser. B*, *52*, 694–716.

Collins, D. R., et al. (2000a), In situ aerosol size distributions and clear-column radiative closure during ACE-2, *Tellus, Ser. B*, *52*, 498–525.

Collins, D. R., H. H. Jonsson, H. Lia, R. C. Flagan, J. H. Seinfeld, K. J. Noone, and S. V. Hering (2000b), Airborne analysis of the Los Angeles aerosol, *Atmos. Environ.*, *34*, 4155–4173.

Cros, B., et al. (2004), An overview of the ESCOMPTE Campaign, *Atmos. Res.*, *69*, 241–279.

de Reus, M., P. Formenti, J. Ström, R. Krejci, D. Müller, M. O. Andreae, and J. Lelieveld (2002), Airborne observations of dry particle absorption and scattering properties over the northern Indian Ocean, *J. Geophys. Res.*, *107*(D22), 8002, doi:10.1029/2002JD002304.

Dubovik, O., A. Smirnov, B. N. Holben, M. D. King, Y. J. Kaufman, T. F. Eck, and I. Slutsker (2000), Accuracy assessments of aerosol optical properties retrieved from Aerosol Robotic Network (AERONET) Sun and sky radiance measurements, *J. Geophys. Res.*, *105*(D8), 9791–9806.

Dubovik, O., B. Holben, T. F. Eck, A. Smirnov, Y. J. Kaufman, M. D. King, D. Tanre, and I. Slutsker (2002), Variability of absorption and optical properties of key aerosol types observed in worldwide locations, *J. Atmos. Sci.*, *59*, 590–608.

Formenti, P., et al. (2002), STAAARTE-MED 1998 summer airborne measurements over the Aegean Sea: 2. Aerosol scattering and absorption, and radiative calculations, *J. Geophys. Res.*, *107*(D21), 4551, doi:10.1029/2001JD001536.

Hansen, J., M. Sato, R. Ruedy, A. Lacis, and V. Oinas (2000), Global warming in the twenty-first century: An alternative scenario, *Proc. Natl. Acad. Sci. U. S. A.*, *97*, 9875–9880.

Hartley, W. S., P. V. Hobbs, J. L. Ross, P. B. Russell, and J. M. Livingston (2000), Properties of aerosols aloft relevant to direct radiative forcing off the mid-Atlantic coast of the United States, *J. Geophys. Res.*, *105*, 9859–9885.

Hegg, A. D., J. Livingston, P. V. Hobbs, T. Novakov, and P. B. Russell (1997), Chemical apportionment of aerosol column optical depth off the mid-Atlantic coast of the United States, *J. Geophys. Res.*, *102*, 25,293–25,303.

Intergovernmental Panel on Climate Change (IPCC) (2001), *Climate Change*, edited by J. T. Houghton et al., Cambridge Univ. Press, New York.

Jokinen, V., and J. M. Mäkelä (1997), Closed-loop arrangement with critical orifice for DMA sheath/excess flow system, *J. Aerosol Sci.*, *28*, 643–648.

Kaufman, Y. J., D. Tanre, and O. Boucher (2002), A satellite view of aerosols in the climate system, *Nature*, *419*, 215–223.

Öström, E., and K. J. Noone (2000), Vertical profiles of aerosol scattering and absorption measured in situ during the North Atlantic Characterization Experiment (ACE-2), *Tellus, Ser. B*, *52*, 526–545.

Raes, F., T. Bates, F. McGovern, and M. VanLiedekerke (2000), The 2nd Aerosol Characterization Experiment (ACE-2), General overview and main results, *Tellus, Ser. B*, *52*, 111–125.

Ramanathan, V., et al. (2001), Indian Ocean Experiment: An integrated analysis of the climate forcing and effects of the great Indo-Asian haze, *J. Geophys. Res.*, *106*, 28,371–28,398.

Roger, J. C., M. Mallet, P. Dubuisson, E. Vermote, H. Cachier, J. P. Putaud, R. Van Dingenen, and S. Despiau (2002), Synergetic approach for the local direct aerosol forcing during the ESCOMPTE campaign, paper presented at Atmospheric Chemistry Within the Earth System, Int. Global Atmos. Chem., Heraklion, Crête.

Russell, P. B., et al. (2002), Comparison of aerosol single scattering albedos derived by diverse techniques in two North Atlantic experiments, *J. Atmos. Sci.*, *59*, 609–619.

Van Dingenen, R., J. P. Putaud, A. Dell'Acqua, S. Martins-Dos Santos, J. Viidanoja, and F. Raes (2002), Physical and chemical aerosol properties at an urban and a rural site during an episode of strong photochemical activity during ESCOMPTE, paper presented at XXVII General Assembly, Eur. Geol. Soc., Nice, France.

Wang, S. C., and R. C. Flagan (1990), Scanning electrical mobility spectrometer, *Aerosol Sci. Technol.*, *13*, 230–240.

H. Cachier, LSCE, Unité mixte CNRS-CEA, Gif sur Yvettte 91 198, France. (helene.cachier@lsce.cnrs-gif.fr)

S. Despiau and M. Mallet, LSEET-LEPI, UMR CNRS 6017, Université du Sud Toulon-Var, La Valette du Var 83162, France. (despiau@isitv.univ-tln.fr; marc.mallet@univ-tln.fr)

J. C. Roger, LOCL/MREN–UMR CNRS ELICO 8013, Université du Littoral Côte d'Opale, Dunkerque, France. (jc@mren2.univ-littoral.fr)

R. Van Dingenen, European Commission, JRC-IES, Climate Change Unit, Ispra I-21020, Italy. (rita.van-dingenen@jrc.it)